ACS Catalysis

Research Article

pubs.acs.org/acscatalysis

Kinetic and Mechanistic Examination of Acid−Base Bifunctional Aminosilica Catalysts in Aldol and Nitroaldol Condensations

Virginia E. Collier, Nathan C. Ellebracht, George I. Lindy, Eric G. Moschetta,* and Christopher W. Jones*

School of Chemical & Biomolecular Engineering Georgia Institute of Technology 311 Ferst Drive NW, Atlanta, Georgia 30332, United States

Supporting Information

ABSTRACT: The kinetic and mechanistic understanding of cooperatively catalyzed aldol and nitroaldol condensations is probed using a series of mesoporous silicas functionalized with aminosilanes to provide bifunctional acid−base character. Mechanistically, a Hammett analysis is performed to determine the effects of electron-donating and electron-withdrawing groups of para-substituted benzaldehyde derivatives on the catalytic activity of each condensation reaction. This information is also used to discuss the validity of previously proposed catalytic mechanisms and to propose a revised mechanism with plausible reaction intermediates. For both reactions, electron-withdrawing groups increase the observed rates of reaction, though resonance effects play an important, yet subtle, role in the nitroaldol condensation, in which a *p*-methoxy electron-donating group is also able to stabilize the proposed carbocation intermediate. Additionally, activation energies and pre-exponential factors are calculated via the Arrhenius analysis of two catalysts with similar amine loadings: one catalyst had silanols available for cooperative interactions (acid−base catalysis), while the other was treated with a silanol-capping reagent to prevent such cooperativity (base-only catalysis). The values obtained for activation energies and pre-exponential factors in each reaction are discussed in the context of the proposed mechanisms and the importance of cooperative interactions in each reaction. The catalytic activity decreases for all reactions when the silanols are capped with trimethylsilyl groups, and higher temperatures are required to make accurate rate measurements, emphasizing the vital role the weakly acidic silanols play in the catalytic cycles. The results indicate that loss of acid sites is more detrimental to the catalytic activity of the aldol condensation than the nitroaldol condensation, as evidenced by the significant decrease in the pre-exponential factor for the aldol condensation when silanols are unavailable for cooperative interactions. Cooperative catalysis is evidenced by significant changes in the pre-exponential factor, rather than the activation energy for the aldol condensation.

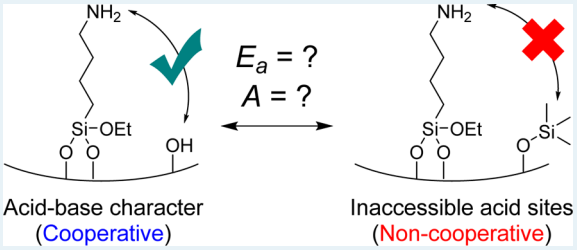

KEYWORDS: *cooperative catalysis, bifunctional acid−base catalysts, Hammett analysis, Arrhenius analysis, condensation reactions, carbon−carbon coupling*

INTRODUCTION

In organic synthesis, the formation of carbon−carbon bonds is an essential step in the production of complex molecules in the fine chemical and pharmaceutical industries.[1−3] These reactions often require homogeneous transition-metal catalysts, which are expensive, can deactivate and/or deteriorate over time, and are difficult to separate and recycle from the reaction mixture.[4−6] Silica-tethered organocatalysts are chemically customizable, are easily separated, and do not require transition metals for several important condensation reactions.[7] The design of these organocatalytic mesoporous silicates is inspired by enzymatic catalysts, in which the functional groups contained in the overall enzyme structure are carefully spaced apart and conform to the substrate, stabilizing the transition state and reducing the required activation energy.[8,9] Heterogeneous bifunctional catalysts, materials that contain two disparate catalytic entities, often act as cooperative catalysts, by which the two species operate in concert to increase the overall rate of reaction in such a fashion that would not be achievable using either of the catalytic species independently.[7] The active species found on the surfaces of bifunctional catalysts often must be kept spatially separated such that they do not negate each other's effects (i.e., acids and bases), as they would in solution, while still allowing them to interact favorably.[7] Mesoporous silica is a popular choice for a support because the surface silanols act as weak Brønsted acids, making them viable as acid partners in acid−base cooperative catalysts.[10−27] Additionally, the range of alkoxysilanes that can be grafted to the native silanols allows for a highly tunable series of organic moieties that can be tethered to the surface to catalyze the desired reaction.[10,11,22,27] A further understanding of these materials has led to practical developments using supported organocatalysts, such as upgrading biomass-derived molecules to materials that may be used as alternative fuel sources, which illustrates their promise as catalysts for important chemical transformations.[17,28]

Received: October 25, 2015
Revised: December 8, 2015
Published: December 9, 2015

DOI: 10.1021/acscatal.5b02398
ACS Catal. 2016, 6, 460−468

Previous work on cooperative acid−base catalysts investigated the physical (e.g., alkyl linker length, pore diameter, arrangement of acids and bases) and chemical properties (e.g., types and strengths of acid and base sites) of such materials to understand the fundamental interactions occurring in the catalytic mechanisms. Brunelli et al. found that aminopropyl (C3) linkers offered high activity (turnover frequency, TOF) for the aldol condensation compared to alkyl linkers with fewer methylene units, while increasing the alkyl linker length past C3 did not increase the observed activity.[23] Later work showed that as the pore diameter of the silica changed, the required alkyl linker length to achieve the maximum TOF for aldol and nitroaldol reactions also changed.[24] Lauwaert et al. examined the effect of the silanol to amine ratio for the aldol condensation and obtained the maximum TOF for a ratio of 1.7.[25] Sharma et al. studied the effect of the total aminosilane loading on MCM-41 silica for the nitroaldol condensation and found that TOFs were highest for loadings between 0.8 and 1.5 mmol of N/g of silica.[29] Another study demonstrated that spacing between silanols and secondary amines on SBA-15 materials could be tuned by changing the calcination temperature of the silica, which affected the concentration and acid strength of the silanols.[16] Several studies have examined the impact of acid strength and spatial organization on cooperative catalysis, noting that weaker acids such as silanols were best at promoting acid−base cooperativity with primary amines.[7,17,22,27,30] Moschetta et al. examined the effect of incorporating heteroatoms into the silica framework and showed that slight increases in the number of Lewis acid sites increased the catalytic activity for the nitroaldol condensation but not the aldol condensation.[30] Shylesh et al. studied the gas-phase self-condensation of butanal over heteroatom-doped SBA-15 silicas functionalized with secondary amines and observed increased catalytic activity for samples containing stronger Brønsted acid sites.[14] These studies suggest that the optimal acid strength depends on the nature of the amine grafted on the surface, as well as the specifics of the coupling reaction, with aldol and nitroaldol reactions showing different trends.

However, additional challenges remain in understanding the mechanisms operating in these condensation reactions using bifunctional catalysts. For example, the aldol and nitroaldol condensations are often used to study the activity of acid−base catalysts, but such studies typically consider one reaction or the other, not both, which makes cross-comparisons difficult.[20,25,29] Kandel et al. spectroscopically verified the formation of stable imines on primary amine-functionalized silica surfaces in the presence of aldol condensation substrates, confirming the role of imines, specifically aldimines resulting from amines reacting with aldehydes, as off-cycle species that inhibited the observed rates of reaction.[31] Another study examined different types of secondary amines on propylsilanes, noting that only a methylamine catalyst had an increased activity in the aldol condensation in comparison to the primary amine.[26] For the aldol condensation, Brunelli et al. postulated sequential activation of the ketone (electrophile) to form the reactive enamine intermediate using a single silanol, which then attacks the aldehyde.[23] One proposed mechanism of the nitroaldol condensation involves simultaneous activation of the reactants and uses multiple silanols.[24] Other studies have proposed mechanisms involving imine intermediates resulting from nucleophilic attack by the amine on the carbonyl group of the aldehyde with subsequent nucleophilic attack of the nitro-containing molecule.[32−35]

In spite of these advances in the design of heterogeneous cooperative aminosilica catalysts, there are still important areas that must be explored to provide key information needed for future catalyst and reaction design. While the above studies have elucidated some key intermediates and offered suggestions for improving bifunctional catalyst design, little has been reported regarding the activation energies and pre-exponential factors of the aldol and nitroaldol condensations using acid−base catalysts.[24] Such information would provide critical information regarding (i) a more quantifiable way to assess the importance of the availability of the silanols as acid partners for the amines via changes in the pre-exponential factors and (ii) possible effects on the transition state by examining changes in the activation energies in each reaction. Furthermore, calculating the activation energies and pre-exponential factors will reveal if molecular collisions (pre-exponential factor) or surpassing a reaction activation barrier has the more significant effect in these catalytic reactions. To this end, in this work, the physical chemistry of the aldol and nitroaldol condensations is explored using MCM-41, a mesoporous silica, functionalized with (4-aminobutyl)triethoxysilane. First, Hammett analysis was performed using the same catalyst for both the aldol and nitroaldol condensations to determine the effects of electron-donating and electron-withdrawing groups on the rates of reaction and the nature of potential reaction intermediates. Additionally, Arrhenius analysis was performed for the aldol and nitroaldol condensations to calculate the observed activation energies and pre-exponential factors. This analysis was repeated for a catalyst at a similar amine loading that contained trimethylsilyl-capped silanols, reducing the cooperative interactions of the silanols with the amines. Comparing the activation energies and pre-exponential factors for both condensation reactions using the catalysts with uncapped and capped silanols has provided quantitative insight into the mechanisms of the cooperative catalytic reactions. Such information can be useful in tailoring the design of future cooperative catalysts.

EXPERIMENTAL SECTION

Materials. Acetone (99.5%), hexane (98.5%), and toluene (99.5%) were purchased from BDH. The aminosilane (4-aminobutyl)triethoxysilane (95%) was purchased from Gelest, 4-nitrobenzaldehyde (99%) and ammonia (28 wt %) were purchased from Alfa Aesar, 1,4-dimethoxybenzene (99%) was procured from Tokyo Chemical Industry (TCI), and cetyltrimethylammonium bromide (CTAB) (99%) was purchased from Acros. Nitromethane (95%), tetraethyl orthosilicate (TEOS; 98%), 4-bromobenzaldehyde (99%), benzaldehyde (98%), 4-methoxybenzaldehyde (98%), 4-methylbenzaldehyde (97%), and hexamethyldisilazane (HMDS, 99.9%) were purchased from Sigma-Aldrich. Ethanol (100%) was obtained from Koptec, and $CDCl_3$ (99.8%) was obtained from Cambridge Isotope Laboratories, Inc.

Synthesis of MCM-41. MCM-41 was synthesized according to a previous report.[24] Cetyltrimethylammonium bromide (7.6 mmol) was dissolved in distilled water (121 mL) with an aqueous ammonia solution (28 wt %, 8.5 g) in a 250 mL flask at room temperature. The mixture was stirred vigorously. TEOS (10 g) was added dropwise, and the mixture was stirred for 2 h. The mixture was filtered and washed several times with distilled water, and the powder was dried at 75 °C in an oven overnight.

DOI: 10.1021/acscatal.5b02398
ACS Catal. 2016, 6, 460−468

The powder was calcined under a flow of air, ramped from room temperature to 550 °C at 1.2 °C/min, held at 550 °C for 12 h, and then cooled to room temperature (10 °C/min). The powder was dried overnight at 200 °C under reduced pressure (10 mTorr).

Grafting of (4-Aminobutyl)triethoxysilane on MCM-41. Silica samples were dried in 100 mL flasks under vacuum at 100 °C overnight. Under nitrogen pressure, the desired amount of (4-aminobutyl)triethoxysilane was added to 500 mg of dried silica in 12.5 mL of anhydrous toluene. Silica samples were stirred at room temperature for 24 h and then heated to 80 °C in an oil bath and reacted for 24 h. The samples were washed, filtered with 100 mL each of toluene, hexane, and ethanol, and then dried under vacuum at 100 °C overnight. The amine loading was measured by elemental analysis (EA), and the results are given in Table 1. In this paper, the naming scheme

Table 1. Textural Properties of the Parent MCM-41 Silica and the Resulting Aminosilica Bifunctional Catalysts

material	surface area (m^2/g)[a]	total pore volume (cm^3/g)[a]	pore diameter (nm)[a]	amine loading (mmol of N/g of silica)[b]
MCM-41	1109	0.97	2.9	
MCM-C4-0.44-H	970	0.78	2.7	0.44
MCM-C4-0.57-A	965	0.76	2.7	0.57
MCM-C4-0.57-A-HMDS	802	0.60	2.4	0.57

[a]Determined by nitrogen physisorption experiments at 77 K. [b]Amine loadings determined by elemental analysis.

for the aminosilica catalysts follows the convention "MCM-C4-*n*-X", where C4 refers to the length of the aminobutyl linker, *n* is the amine loading in mmol of N/g of silica, and X refers to whether the catalyst was used in the Hammett (H) or Arrhenius analysis (A). The catalyst that was treated with HMDS has "HMDS" at the end of its name.

Materials Characterization. All nitrogen physisorption experiments were conducted on a Micromeritics Tristar 2030 instrument at 77 K. All samples were evacuated for at least 12 h at 110 °C using at least 100 mg of each material. The nitrogen uptake isotherms were analyzed using the Brunauer–Emmett–Teller (BET) method to calculate the surface area of each material and the Broekhoff–de Boer method with the Frenkel–Halsey–Hill (BdB-FHH) modification using the data from the adsorption isotherm to calculate the cumulative pore volume and the pore diameter.[36] X-ray diffraction (XRD) experiments were performed on a PAnalytical X'Pert diffractometer using a Cu Kα X-ray source. Samples were scanned at a grazing angle of 1° and a step size of 0.02° over a 2θ range of 1–10°. All samples were sent to Atlantic Microlabs (Norcross, GA) for CHN elemental analysis (EA). All ^{1}H NMR spectra of the crude mixtures of the nitroaldol condensation products were recorded on a Bruker DMX 400 spectrometer using $CDCl_3$ as the solvent. No dinitroalkane products were observed in any of the crude mixtures.[37] Transmission electron microscopy (TEM) of the MCM-41 can be found in Figure S6 of the Supporting Information, and other microscopy images can be found in a previous report.[24]

General Catalytic Experiments for MCM-41 Materials with Uncapped Silanols. For each aldol condensation, 2 mL of reaction solution containing 0.05 M 4-nitrobenzaldehyde as reactant and 0.05 M 1,4-dimethoxybenzene as an internal standard in acetone was added to a clean 25 mL two-neck flask with a magnetic stir bar. Next, 10 mol % of catalyst (by amine loading) was added to the reaction solution and the reaction was run in an oil bath at 50 °C under a condenser with an atmosphere of nitrogen. Samples were taken every 15 min for the first 1 h and then one sample per hour for a total of 4 h. All reactions were performed three times to ensure reproducibility, and the average conversion values of the reactions were used to calculate TOFs during the first 1 h of reaction (the conversion data as a function of time were linear in this region). For each nitroaldol condensation, 1 mL of reaction solution containing 0.05 M 4-nitrobenzaldehyde as reactant and 0.05 M 1,4-dimethoxybenzene as an internal standard in nitromethane was placed in a clean 25 mL two-neck flask with a magnetic stir bar. Next, 10 mol % of catalyst (by amine loading) was added to the reaction solution and the reaction was run in an oil bath at 40 °C under a condenser with an atmosphere of nitrogen. Samples were taken every 15 min for the first 1 h and then one sample per hour for a total of 4 h. All reactions were performed three times to ensure reproducibility, and the average conversion values of the reactions were used to calculate TOFs during the first 1 h of reaction (once again, the conversion data as a function of time were linear). Reactant conversions were determined by GC (Shimadzu GC-2010) with a flame ionization detector (FID), an autoinjector and autosampler (AOC-20i+s model), and an Agilent DB-1701 column (30 m, 0.25 mm inner diameter, 0.25 μm film thickness).

Hammett Analysis. The Hammett reaction setup was replicated as detailed above using MCM-C4-0.44-H and one of five different para-substituted benzaldehyde derivatives (4-nitrobenzaldehyde, 4-methoxybenzaldehyde, 4-bromobenzaldehyde, 4-methylbenzaldehyde, and benzaldehyde). Samples for each new reactant were taken every 15 min for 1 h to calculate the TOFs. Each derivative reaction was run three times, and average TOFs are reported. All Hammett substituent constants were taken from a previous review of reported values.[38] The crude reaction mixtures of the nitroaldol condensation were examined by ^{1}H NMR spectroscopy to determine the selectivity, though only the nitrostyrene products were present, in agreement with a previous report.[34]

Arrhenius Analysis. The aldol and nitroaldol condensations were performed as detailed above using MCM-C4-0.57-A as the catalyst and 4-nitrobenzaldehyde as the reactant, varying only the reaction temperature. The aldol reaction was run from 45 to 55 °C, while the nitroaldol condensation was run from 40 to 55 °C. Each set of reactions was performed again using an HMDS-treated catalyst (MCM-C4-0.57-A-HMDS) with a similar amine loading. A portion of MCM-C4-0.57-A catalyst was capped by vigorous mixing with neat HMDS and allowed to react for 24 h at room temperature, resulting in a catalyst with capped silanols. The HMDS-treated catalyst was washed with 100 mL each of toluene, hexanes, and ethanol and dried under vacuum at 100 °C overnight. Due to the presence of the capped silanols, the reaction temperatures were increased for the HMDS-treated catalyst. Four reactions were run in parallel in 10 mL pressure tubes. Each vessel was loaded with a magnetic stir bar, 2.7 mL of reaction solution, and 5 mol % (by amine loading) of capped MCM-C4-0.57-A-HMDS catalyst. The reactions were carried out in pressure tubes to prevent evaporation of solvent from the reaction solution over time, as they required elevated temperatures and increased reaction times to observe measurable conversion values. An aliquot was

DOI: 10.1021/acscatal.5b02398
ACS Catal. 2016, 6, 460–468

taken from each pressure tube prior to heating as the initial time point. For each subsequent time point (every 30 min for nitroaldol, 1 h for aldol), the pressure tubes were removed from the oil bath and cooled in an ice bath for 5 min to reduce solvent vapor escaping the tube upon opening. During this time, the reaction timer was stopped. After aliquots were taken from each vessel, they were placed back in the oil bath and the reaction timer was started after a short delay to allow for temperature equilibration. All conversion data used to calculate TOFs, and therefore activation energies and pre-exponential factors, were linear as a function of time.

RESULTS AND DISCUSSION

Physical and Chemical Characterization of Materials. Nitrogen physisorption was used to characterize the textural properties of the MCM-41 materials, the results of which are reported in Table 1. The adsorption isotherms (Figure 1)

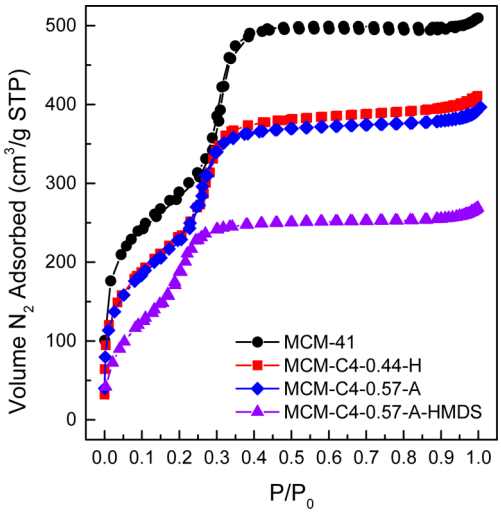

Figure 1. Nitrogen physisorption isotherms of the bare MCM-41 silica and the amine-functionalized MCM-41 silicas used as cooperative catalysts.

revealed the retention of mesoporosity after functionalization with the aminosilanes, indicating the grafting conditions were sufficiently mild. All aminosilica materials had decreased surface areas, pore volumes, and pore diameters in comparison to the parent MCM-41 due to the presence of the grafted aminosilanes. All catalysts were derived from this parent MCM-41 to ensure the materials had similar textural properties, allowing for straightforward comparison of their catalytic behavior. The aminosilica that was treated with HMDS to cap the surface silanols with trimethylsilyl groups (MCM-C4-0.57-A-HMDS) exhibited a decrease in surface area, pore volume, and pore diameter in comparison to the same aminosilica material (MCM-C4-0.57-A) without HMDS treatment, an expected consequence of successful capping of the silanols.

X-ray diffraction (XRD) patterns were obtained for all MCM-41 materials and the patterns are shown in Figure 2. The (100) reflections appeared at $2\theta = 2.3-2.5°$ for all samples, and the (110) and (200) reflections appeared at $2\theta = 4.1-4.8°$, indicating that the 2D hexagonal structure of the parent MCM-41 silica was initially achieved and remained intact on the other materials after grafting and HMDS treatment, where appropriate.[39,40] The nitrogen content of each catalyst was determined by EA and is summarized in Table 1. Samples

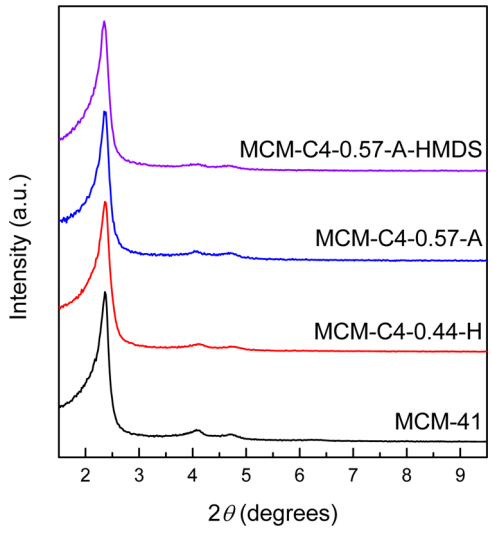

Figure 2. XRD patterns of the bare MCM-41 silica and the amine-functionalized MCM-41 silicas, showing the (100), (110), and (200) reflections in all cases.

with increased aminosilane loadings had decreased surface areas, pore volumes, and pore diameters, which is consistent with the filling the pores of the MCM-41 silica with the aminosilanes.

Hammett Analysis of Cooperative Catalysts. The reaction schemes for the aldol and nitroaldol condensations are presented in Scheme 1, and the results of the Hammett analysis for the aldol condensation are presented in Figure 3. The TOF values for the five benzaldehyde derivatives were best fit using the standard σ values, the substituent constants, with a slope of 0.78, indicating a moderate substituent effect on the activity of the reaction.[38] The positive value of the slope revealed that electron-withdrawing groups at the para position on the benzaldehyde accelerated the rate of reaction in the case of the aldol condensation.[38] Including electron-withdrawing groups at the para position decreases the electron density at the carbonyl group of the aldehyde, increasing its electrophilicity and making the aldehyde more susceptible to nucleophilic attack. This observation is consistent with the proposed mechanism of the aldol condensation, illustrated in Scheme 2.[23,25,26] The key step in the mechanism is the nucleophilic attack of the enamine, generated by activation of the acetone, on the aldehyde interacting with a surface silanol.[23,25,26] This step provides a reasonable explanation for why increasing the electrophilicity of the aldehyde via incorporation of electron-withdrawing groups led to increased TOF values in the aldol condensation.

Conversely, the Hammett analysis for the nitroaldol condensation revealed interesting differences in comparison to the aldol condensation, as shown in Figure 4. First, the slope of the fit is also positive, but the magnitude of the slope is reduced in comparison to the aldol condensation. This decreased slope would seem to suggest that substituent effects do not have a significant effect on the observed kinetics of the nitroaldol condensation, but closer inspection reveals a subtle stabilization effect based on the electronic nature of the substituent. Second, the results of the nitroaldol condensation using the five benzaldehyde derivatives were best fit using σ^+ values, which have different physical meanings in comparison to traditional σ values (see Figure S1 in the Supporting

DOI: 10.1021/acscatal.5b02398
ACS Catal. 2016, 6, 460−468

Scheme 1. General Reaction Schemes for (A) the Aldol Condensation and (B) the Nitroaldol Condensation[a]

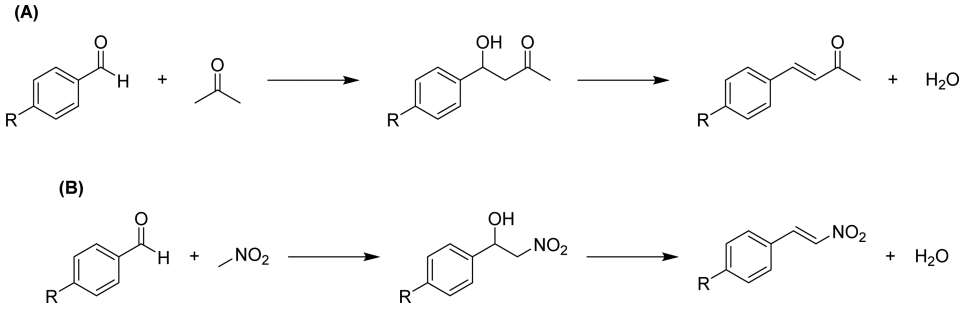

[a]The dinitroalkane side product in the nitroaldol condensation[37] was not observed by ^{1}H NMR spectroscopy and is not presented in this scheme.

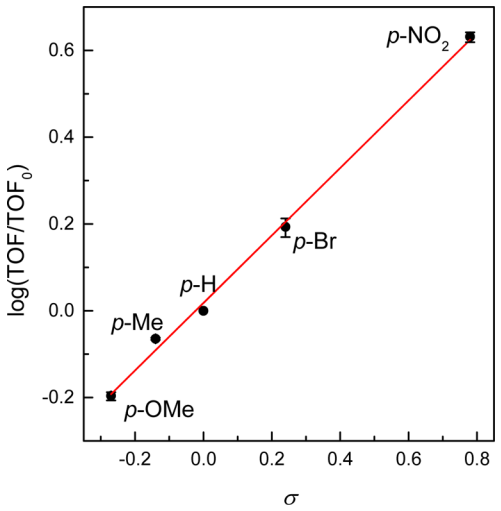

Figure 3. Hammett plot for para-substituted benzaldehydes in the aldol condensation with acetone at 50 °C. The TOF values were obtained using the initial rate over the first hour of reaction. The TOF_0 value is the TOF obtained when using the reference benzaldehyde (*p*-H).

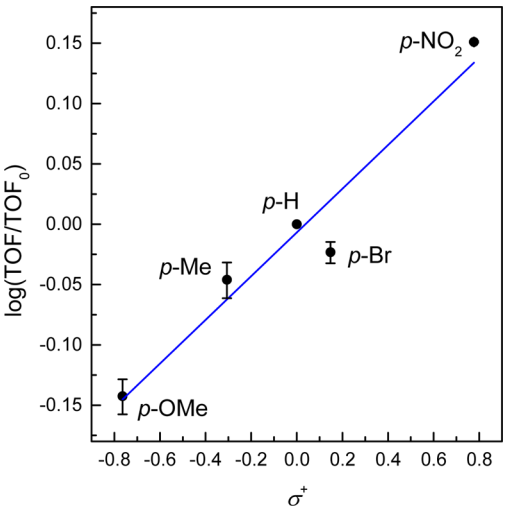

Figure 4. Hammett plot for para-substituted benzaldehydes in the nitroaldol condensation with nitromethane at 40 °C using σ^+ values. The TOF values were obtained using the initial rate over the first hour of reaction. The TOF_0 value is the TOF obtained when using the reference benzaldehyde (*p*-H).

Scheme 2. Proposed Mechanism for the Aldol Condensation of Acetone and Para-Substituted Benzaldehydes on Aminosilica Cooperative Catalysts[a]

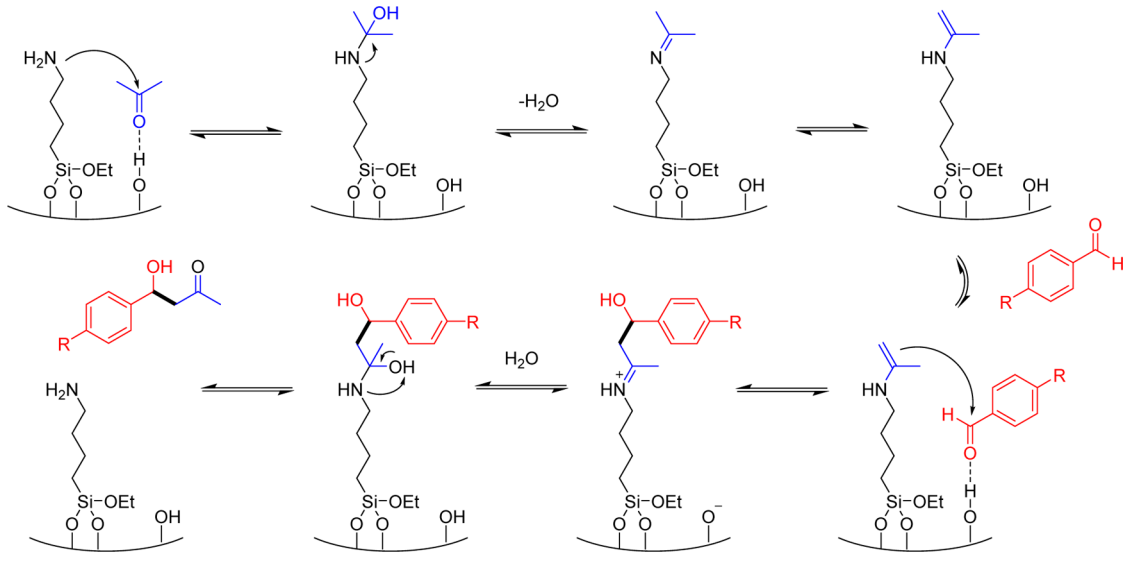

[a]Generation of the nucleophilic enamine leads to attack on the electrophilic carbonyl group of the aldehyde.

DOI: 10.1021/acscatal.5b02398
ACS Catal. 2016, 6, 460−468

Information for the fit using σ values). As Brown and Okamoto observed, these modified substituent constants correlate to cationic species that are generated during the reaction.[41,42] Obtaining a better linear fit of the reactivity data using the σ^+ values indicates the formation of a cationic or near-cationic intermediate or transition state, which suggests that electron-donating groups in the para position may stabilize these cationic intermediates via electron delocalization through the aromatic ring, as will be discussed shortly. A proposed nitroaldol mechanism is presented in Scheme 3, which begins with the alkylamine abstracting one of the acidic protons of a molecule of nitromethane that interacts with a surface silanol. The aldehyde interacts with a second silanol, which allows for simultaneous activation of the reactants, and is subjected to nucleophilic attack at the carbonyl group. The nitroaldol product is formed, and the cycle is complete. This mechanism is plausible and is likely the dominant pathway when electron-withdrawing groups are present in the para position and is consistent with previous observations of electron-withdrawing groups in the nitroaldol condensation as reported by Sharma and co-workers.[32]

Scheme 3. Proposed Mechanism for the Nitroaldol Condensation of Nitromethane and Para-Substituted Benzaldehydes on Aminosilica Cooperative Catalysts[a]

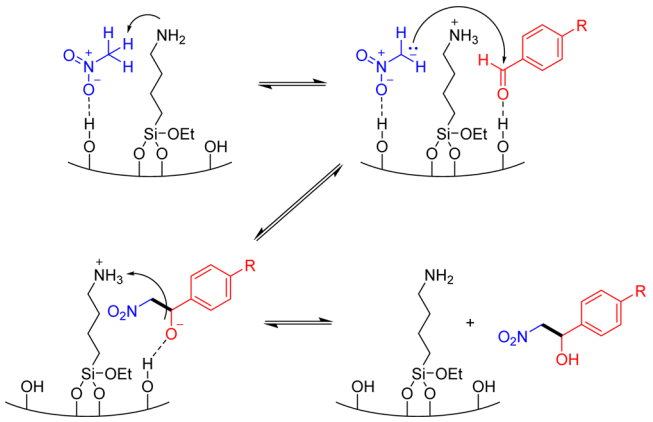

[a]This mechanism postulates the use of two silanols to activate both reactants simultaneously.[24]

However, the Hammett analysis suggests resonance effects from electron-donating groups in the para position. Previous reports suggested the formation of imines via attack of the amines on the aldehydes either when electron-donating groups were used in the para position of the aldehydes or when the silanols were capped with trialkylsilyl groups and unable to participate in cooperative catalysis.[32,33] This mechanism (presented as Scheme S1 in the Supporting Information) is potentially feasible, as is the mechanism in Scheme 3, though the subtle effect of the electron-donating group, specifically *p*-OMe, is further illustrated in Scheme 4. Here, the carbonyl group of the aldehyde is stabilized by a surface silanol, which withdraws electron density from the oxygen atom of the carbonyl group. To compensate for this effect, the silanol-stabilized aldehyde has a resonance structure in which the π electrons of the carbonyl group delocalize to the oxygen atom, generating an alkoxy ion and leaving a cation at the benzylic carbon, which is consistent with the improved fit of the Hammett data using the σ^+ values.[41,42]

When the electron-donating *p*-OMe group is present, it can stabilize the benzylic carbocation via electron delocalization through the aromatic ring, which forms an oxonium ion at the para position. This through-conjugation or through-resonance effect of electron-donating groups stabilizes the carbocation intermediate, which increases the rate of reaction, most likely by reducing the activation energy. The *p*-Me substitution likely does not strongly contribute to a resonance-stabilized form of the aldehyde, even though it is an electron-donating group. The resonance structures in Scheme 4 are drawn with the *p*-OMe group to illustrate the effect of through-resonance. It is possible that both proposed mechanisms (Scheme 3 and Scheme S1 in the Supporting Information) for the nitroaldol condensation proceed simultaneously for all five benzaldehyde derivatives examined, though the dominant mechanism likely depends on the electronic nature of the para substituent.

However, the only data point not to agree with the Hammett analysis using the σ^+ values was the point corresponding to the *p*-Br substitution. In spite of the electron-withdrawing properties of the *p*-Br group, no plausible resonance structures exist that can stabilize a carbocation at the benzylic position. If the substitution is an electron-withdrawing nitro group, plausible resonance structures exist that would stabilize the same carbocation via electron delocalization through the aromatic ring once the carbonyl group hydrogen bonds with the silanol. These results suggest that para substitutions capable of

Scheme 4. Effect of through-Conjugation via Electron Delocalization through the Aromatic Ring of *p*-OMe-Substituted Benzaldehyde[a]

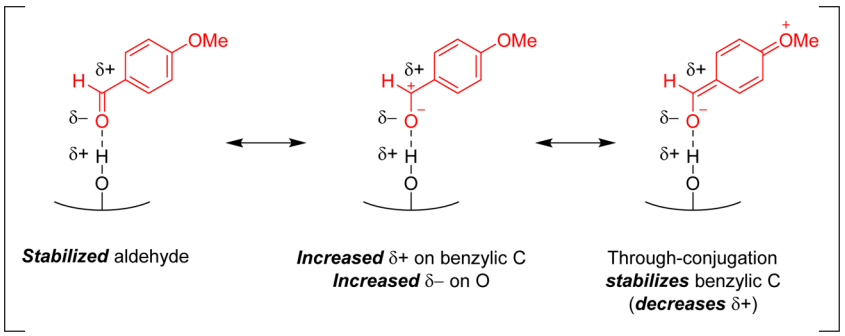

[a]The hydrogen-bonding ability of the silanols stabilizes the aldehyde and withdraws electron density from the carbonyl group, ultimately generating a benzylic carbocation. The *p*-OMe group is shown explicitly in the mechanism to illustrate plausible resonance-stabilized carbocation intermediates.

DOI: 10.1021/acscatal.5b02398
ACS Catal. 2016, 6, 460–468

delocalizing electron density throughout the aromatic ring may accelerate the rate of the nitroaldol condensation, regardless of whether the substitution is electron-donating or electron-withdrawing. This suggestion is supported by the reduced magnitude of the slope of the Hammett plot for the nitroaldol condensation (0.18) in comparison to that of the aldol condensation (0.78). It is better to think of the reduced slope of the Hammett plot in the nitroaldol condensation as the combined effects of electron-donating groups (improved stabilization of the reaction intermediate) and electron-withdrawing groups (increasing the electrophilicity of the aldehyde) both being capable of increasing the rate of reaction, albeit for slightly different reasons, which would lead to the original suggestion that substituents do not have a significant effect on the kinetics. The reduced magnitude of the slope could also reflect changes in the dominant mechanism as the substituent changes, as discussed previously. Furthermore, these results provide reasonable structures for the likely reaction intermediates (i.e., the carbocations). The differences in the Hammett analyses for the aldol and nitroaldol condensations are in agreement with a previous report regarding the incorporation of Brønsted and Lewis acid sites into silica materials by heteroatom substitution.[30] Modest increases in the number of Lewis acid sites were found to increase the catalytic activity for the nitroaldol condensation, but not for the aldol condensation.[30] This effect is consistent with the proposed structures in Scheme 4 because the acid interactions with the carbonyl group of the aldehyde assist the aldehyde with entering the catalytic cycle and help stabilize the resulting carbocation. The acid functionality of the surface, be it through native silanols, heteroatom substitutions, or other acid sources/sites, could help withdraw the electron density from the carbonyl group, making the carbon at the benzylic position more electrophilic, facilitating both through-resonance from electron-donating groups at the para position and easier nucleophilic attack at the carbocation. Conversely, stabilizing the aldehyde in the aldol condensation would promote the nucleophilic attack of the aldehyde by the amine to form an imine (a secondary aldimine), rendering the amine less active for catalysis because the acetone would be unable to react with the resulting imine.[31] In this case, the aldimine cannot form a nucleophilic enamine because there are no α protons available on the aldimine, which bears an aryl substituent, resulting in the aldimine being a catalytically inactive off-cycle species.[31] Unlike deprotonated nitromethane, which can react with the aldimine in the nitroaldol condensation to form the product as shown in Scheme S1 in the Supporting Information, acetone cannot be activated in such a way to make it a better nucleophile; thus, if the amines preferentially attack the acid-stabilized aldehyde in the aldol condensation, the catalytic activity should decrease.

Arrhenius Analysis of Cooperative Catalysts. Arrhenius analysis of an aminosilica catalyst with available silanols (MCM-C4-0.57-A) and with trimethylsilyl-capped silanols (MCM-C4-0.57-A-HMDS) revealed very useful mechanistic insight into the aldol and nitroaldol condensations from the obtained activation energies and pre-exponential factors reported in Table 2. All Arrhenius plots are presented in Figures S2−S5 in the Supporting Information, and the TOFs are reported in Tables S1 and S2 in the Supporting Information. For the aldol condensation, the activation energy and the pre-exponential factor decreased once the silanols were capped with trimethylsilyl groups. The observed decrease in activation energy could be due to the presence of different reaction intermediates as a consequence of the silanols being unavailable for cooperative interactions. However, it should be noted that the TOF values for the trimethylsilyl-capped catalysts decreased in comparison to the catalysts with available silanols and required higher reaction temperatures to achieve any appreciable conversion, further emphasizing the importance of the silanols for cooperative interactions. As an interesting finding, a significant decrease in the pre-exponential factor caused the reaction rate to decrease in spite of the decreased activation energy, providing additional compelling evidence of the vital role that cooperative acid−base interactions serve in the aldol condensation. The pre-exponential factor depends on the total number of molecular collisions occurring over the course of the reaction, meaning that as the value of the pre-exponential factor increases, it is more likely that reactant molecules, most likely including cocatalytic amines and silanols, are colliding with one another in productive ways with greater frequency.[43] After the silanols are capped, the reaction has a similar or even lower energy transition state, but the likelihood of reaching that state by productive collisions is far lower due to the lack of available silanols, which were previously abundantly present. In this regard, capping the silanols significantly decreased the pre-exponential factor because the acid sites were unable to promote the activation of acetone and likely led to the amines attacking the aldehyde, forming unproductive imines (secondary aldimines) from the aldehydes, decreasing the number of available amines in the catalytic cycle. These results are also consistent with previous reports in which stronger acid sites decreased the catalytic activity of aminosilicates in the aldol condensation, in the sense that substituting stronger acid sites for the inherently weaker silanols decreased the observed rates of reaction, but some acids were necessary to achieve appreciable conversion.[10,11,22,27,30] Another possible interpretation of the reduced activation energy is that the reduced value reflects the direct nucleophilic attack of the acetone by the amines without the assistance of the silanols. If a silanol is present, it will hydrogen bond with the acetone, meaning that the energy of the hydrogen bond must be accounted for in the activation of the acetone by the amine. Without available silanols, this hydrogen bond does not need to be disrupted, which could explain why the activation energy decreased for the aldol condensation after capping the silanols. This direct acetone activation pathway is consistent with the decreased pre-exponential factor, because the number of direct molecular interactions of the amines with the acetone molecules likely would be reduced dramatically without silanols available for cooperative interactions.

The Arrhenius analysis for the nitroaldol conversion further revealed differences between the two condensation reactions. The obtained activation energies and pre-exponential factors were only slightly decreased for the aminosilica catalysts with capped silanols in comparison to the catalysts with available silanols, indicating that the loss of the acid functionality of the

Table 2. Activation Energies, E_a, and Pre-Exponential Factors, A, for the Aldol and Nitroaldol Condensations Using Catalysts with and without Accessible Silanols

material	reaction	E_a (kJ/mol)	A (s^{-1})
MCM-C4-0.57-A	aldol	40.1	9.33×10^6
MCM-C4-0.57-A-HMDS	aldol	28.9	4.03×10^4
MCM-C4-0.57-A	nitroaldol	51.3	8.52×10^8
MCM-C4-0.57-A-HMDS	nitroaldol	43.5	6.36×10^8

DOI: 10.1021/acscatal.5b02398
ACS Catal. 2016, 6, 460−468

surface was not as severe as in the case of the aldol condensation. At first, this notion would seem to be counterintuitive on the basis of the evidence that increased numbers of acid sites have been shown to increase the activity in the nitroaldol condensation,[30] but other observations may lead to a plausible explanation. First, the nitroaldol condensation may readily proceed via a base-catalyzed mechanism in which no acid components are necessary to complete the catalytic cycle.[33−35] This proposed mechanism involves the formation of an imine intermediate via condensation of the aldehyde with an amine with subsequent attack of the deprotonated nitromethane on the imine to form the nitroaldol product (see Scheme S1 in the Supporting Information).[33−35] In contrast, the aldol condensation requires activation of the acetone and subsequent attack of the enamine on the carbonyl of the aldehyde. If the amines dehydrate the aldehyde first, the resulting imine most likely would be unable to react with the acetone molecules present in solution, meaning that a base-only mechanism likely would not effectively promote the aldol condensation using aminosilica catalysts with capped silanols (i.e., without acid sites).[31] This mechanism would also explain why capping the silanols was severely detrimental to the aldol condensation yet not as disadvantageous to the activity of the nitroaldol condensation. Most likely, the array of proposed mechanisms of the nitroaldol condensation operate simultaneously and not all of them require silanols or they can use other acid sources; thus, when the silanols are capped, there are alternative pathways for the reaction to proceed in the absence of silanols.

Previous work demonstrated that changing the alkylamine linker length and the pore diameter of the silica (i.e., the curvature of the surface) had a stronger effect on the observed TOFs for the nitroaldol condensation than for the aldol condensation.[24] With the results of the present work, these linker length and surface curvature effects might be viewed as a likely consequence of allowing each available alkylamine to interact with a larger total number of available silanols, which would have a more pronounced effect on the nitroaldol condensation (two possible silanol-assisted pathways) in comparison to the aldol condensation (one silanol-assisted pathway). As with the aldol condensation, it should be noted that the TOF values decreased using the catalyst with the capped silanols in comparison to the catalyst without capped silanols and elevated temperatures were required to achieve appreciable conversion. The larger decrease in the pre-exponential factor for the aldol condensation when the silanols were unavailable for cooperative interactions suggests that the aldol condensation is more dependent on the amines and the silanols being fully accessible to facilitate cooperative molecular collisions between the reactants in comparison to the nitroaldol condensation.

CONCLUSIONS

The kinetics and mechanisms of cooperatively catalyzed aldol and nitroaldol condensations using amine-functionalized MCM-41 mesoporous silicas as bifunctional acid−base catalysts were examined using Hammett and Arrhenius analyses. From the Hammett analysis of the aldol condensation, electron-withdrawing para substituents on benzaldehyde were found to accelerate of the rate of the reaction. This observation was consistent with the proposed mechanism, in which the carbonyl of the aldehyde is subjected to nucleophilic attack by an enamine, which would be accelerated by para substituents withdrawing electron density from the carbonyl group via the aromatic ring. Conversely, in the nitroaldol condensation, the *p*-OMe electron-donating group provided additional stability to the intermediate carbocation generated at the benzylic position via through-resonance in the form of electron delocalization through the aromatic ring. Arrhenius analysis of the two condensations revealed a stronger dependence of the pre-exponential factor for the aldol condensation, owing to the difficulty of activating the acetone molecules in the presence of capped silanols on the silica surface (i.e., loss of acid character), suggesting that the amines and silanols were both necessary to promote molecular collisions necessary for cooperative catalysis. However, capping the silanols with trimethylsilyl groups for all reactions required elevated temperatures to achieve appreciable conversion and reduced the observed TOF values in comparison to materials with available silanols, further emphasizing the importance of the silanols as weak acid partners in cooperative catalysis.

ASSOCIATED CONTENT

Supporting Information

The Supporting Information is available free of charge on the ACS Publications website at DOI: 10.1021/acscatal.5b02398.

Hammett plot of the nitroaldol reactivity data using σ values, the base-only nitroaldol mechanism that operates via imine intermediate, Arrhenius plots and TOFs, and a TEM image of the MCM-41 (PDF)

AUTHOR INFORMATION

Corresponding Authors

*E-mail for E.G.M.: eric.moschetta@chbe.gatech.edu.
*E-mail for C.W.J.: cjones@chbe.gatech.edu.

Notes

The authors declare no competing financial interest.

ACKNOWLEDGMENTS

This work was supported by the Department of Energy Office of Basic Energy Sciences through Catalysis Contract No. DEFG02-03ER15459. The authors thank Dr. Li-Chen Lee and Ms. Caroline Hoyt for helpful discussions, Dr. Li-Chen Lee for performing the NMR experiments, and Dr. Simon Pang for taking the TEM image. The authors thank a reviewer for particularly insightful comments.

REFERENCES

(1) Trost, B. M. *Angew. Chem., Int. Ed. Engl.* **1995**, *34*, 259−281.
(2) Ritleng, V.; Sirlin, C.; Pfeffer, M. *Chem. Rev.* **2002**, *102*, 1731−1770.
(3) Colby, D. A.; Bergman, R. G.; Ellman, J. A. *Chem. Rev.* **2010**, *110*, 624−655.
(4) Tsubogo, T.; Ishiwata, T.; Kobayashi, S. *Angew. Chem., Int. Ed.* **2013**, *52*, 6590−6604.
(5) Finelli, F. G.; Miranda, L. S. M.; de Souza, R. O. M. A. *Chem. Commun.* **2015**, *51*, 3708−3722.
(6) Vural Gürsel, I.; Noël, T.; Wang, Q.; Hessel, V. *Green Chem.* **2015**, *17*, 2012−2026.
(7) Margelefsky, E. L.; Zeidan, R. K.; Davis, M. E. *Chem. Soc. Rev.* **2008**, *37*, 1118−1126.
(8) Bornscheuer, U. T.; Huisman, G. W.; Kazlauskas, R. J.; Lutz, S.; Moore, J. C.; Robins, K. *Nature* **2012**, *485*, 185−194.
(9) Warshel, A.; Sharma, P. K.; Kato, M.; Xiang, Y.; Liu, H.; Olsson, M. H. M. *Chem. Rev.* **2006**, *106*, 3210−3235.

DOI: 10.1021/acscatal.5b02398
ACS Catal. 2016, 6, 460−468

(10) Zeidan, R. K.; Hwang, S. J.; Davis, M. E. *Angew. Chem., Int. Ed.* **2006**, *45*, 6332−6335.
(11) Zeidan, R. K.; Davis, M. E. *J. Catal.* **2007**, *247*, 379−382.
(12) Shylesh, S.; Wagener, A.; Seifert, A.; Ernst, S.; Thiel, W. R. *ChemCatChem* **2010**, *2*, 1231−1234.
(13) Shylesh, S.; Thiel, W. R. *ChemCatChem* **2011**, *3*, 278−287.
(14) Shylesh, S.; Hanna, D.; Gomes, J.; Canlas, C. G.; Head-Gordon, M.; Bell, A. T. *ChemSusChem* **2015**, *8*, 466−472.
(15) Hanna, D. G.; Shylesh, S.; Li, Y.-P.; Krishna, S.; Head-Gordon, M.; Bell, A. T. *ACS Catal.* **2014**, *4*, 2908−2916.
(16) Shylesh, S.; Hanna, D.; Gomes, J.; Krishna, S.; Canlas, C. G.; Head-Gordon, M.; Bell, A. T. *ChemCatChem* **2014**, *6*, 1283−1290.
(17) Shylesh, S.; Sreekumar, S.; Gomes, J.; Grippo, A.; Arab, G. E.; Head-Gordon, M.; Toste, F. D.; Bell, A. T. *Angew. Chem., Int. Ed.* **2015**, *54*, 4673−4677.
(18) Gianotti, E.; Diaz, U.; Velty, A.; Corma, A. *Catal. Sci. Technol.* **2013**, *3*, 2677−2688.
(19) Díaz, U.; Brunel, D.; Corma, A. *Chem. Soc. Rev.* **2013**, *42*, 4083−4097.
(20) Bass, J. D.; Solovyov, A.; Pascall, A. J.; Katz, A. *J. Am. Chem. Soc.* **2006**, *128*, 3737−3747.
(21) Hruby, S. L.; Shanks, B. H. *J. Catal.* **2009**, *263*, 181−188.
(22) Brunelli, N. A.; Venkatasubbaiah, K.; Jones, C. W. *Chem. Mater.* **2012**, *24*, 2433−2442.
(23) Brunelli, N. A.; Didas, S. A.; Venkatasubbaiah, K.; Jones, C. W. *J. Am. Chem. Soc.* **2012**, *134*, 13950−13953.
(24) Brunelli, N. A.; Jones, C. W. *J. Catal.* **2013**, *308*, 60−72.
(25) Lauwaert, J.; De Canck, E.; Esquivel, D.; Thybaut, J. W.; Van Der Voort, P.; Marin, G. B. *ChemCatChem* **2014**, *6*, 255−264.
(26) Lauwaert, J.; De Canck, E.; Esquivel, D.; Van Der Voort, P.; Thybaut, J. W.; Marin, G. B. *Catal. Today* **2015**, *246*, 35−45.
(27) Lauwaert, J.; Moschetta, E. G.; Van Der Voort, P.; Thybaut, J. W.; Jones, C. W.; Marin, G. B. *J. Catal.* **2015**, *325*, 19−25.
(28) Balakrishnan, M.; Sacia, E. R.; Bell, A. T. *ChemSusChem* **2014**, *7*, 1078−1085.
(29) Sharma, K. K.; Buckley, R. P.; Asefa, T. *Langmuir* **2008**, *24*, 14306−14320.
(30) Moschetta, E. G.; Brunelli, N. A.; Jones, C. W. *Appl. Catal., A* **2015**, *504*, 429−439.
(31) Kandel, K.; Althaus, S. M.; Peeraphatdit, C.; Kobayashi, T.; Trewyn, B. G.; Pruski, M.; Slowing, I. I. *J. Catal.* **2012**, *291*, 63−68.
(32) Sharma, K. K.; Biradar, A. V.; Asefa, T. *ChemCatChem* **2010**, *2*, 61−66.
(33) Bass, J. D.; Solovyov, A.; Pascall, A. J.; Katz, A. *J. Am. Chem. Soc.* **2006**, *128*, 3737−3747.
(34) Demicheli, G.; Maggi, R.; Mazzacani, A.; Righi, P.; Organica, C.; Mangini, A. *Tetrahedron Lett.* **2001**, *42*, 2401−2403.
(35) Zorn, D.; Lin, V. S. Y.; Pruski, M.; Gordon, M. S. *J. Phys. Chem. A* **2008**, *112*, 10635−10649.
(36) Lukens, W. W.; Schmidt-Winkel, P.; Zhao, D.; Feng, J.; Stucky, G. D. *Langmuir* **1999**, *15*, 5403−5409.
(37) Motokura, K.; Tada, M.; Iwasawa, Y. *Angew. Chem., Int. Ed.* **2008**, *47*, 9230−9235.
(38) Hansch, C.; Leo, A.; Taft, R. W. *Chem. Rev.* **1991**, *91*, 165−195.
(39) Kresge, C. T.; Leonowicz, M. E.; Roth, W. J.; Vartuli, J. C.; Beck, J. S. *Nature* **1992**, *359*, 710−712.
(40) Kruk, M.; Jaroniec, M.; Kim, J. M.; Ryoo, R. *Langmuir* **1999**, *15*, 5279−5284.
(41) Brown, H. C.; Okamoto, Y. *J. Am. Chem. Soc.* **1957**, *79*, 1913−1917.
(42) Brown, H. C.; Okamoto, Y. *J. Am. Chem. Soc.* **1958**, *80*, 4979−4987.
(43) Moore, J. W.; Pearson, R. G. In *Kinetics and Mechanism*; Wiley: New York, 1981; pp 116−121.

DOI: 10.1021/acscatal.5b02398
ACS Catal. 2016, 6, 460−468